Using biomarkers as fingerprint properties to identify sediment sources in a small catchment

Fangxin Chen [a,c], Nufang Fang [a,b,*], Zhihua Shi [a,c]

[a] State Key Laboratory of Soil Erosion and Dryland Farming on the Loess Plateau, Northwest A & F University, Yangling 712100, PR China
[b] Institute of Soil and Water Conservation of Chinese Academy of Sciences and Ministry of Water Resources, Yangling 712100, PR China
[c] College of Resources and Environment, Huazhong Agricultural University, Wuhan 430070, China

HIGHLIGHTS

- *n*-Alkanes as a new fingerprinting method was used to identify sediment sources.
- Using genetic algorithm finds the best optimum source contribution to sediments.
- Biological and geochemical fingerprinting was used in this study.
- The young forest is the main sediment source.

GRAPHICAL ABSTRACT
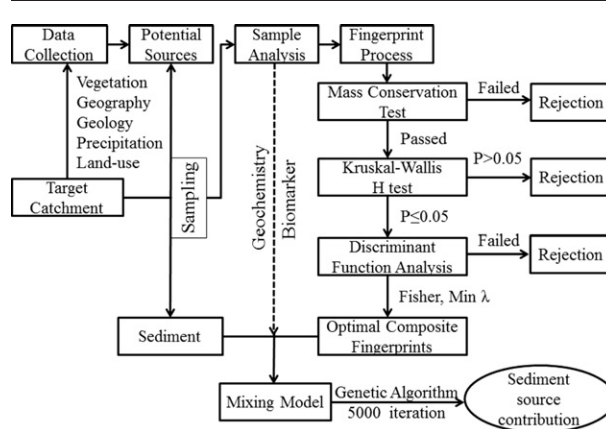
ABSTRACT

Traditional fingerprinting methods are limited in their ability to identify soil erosion sources where geologic variations are small or where different land uses span geological boundaries. In this study, a new biomarker for fingerprinting, specifically, *n*-alkanes, was used in a small catchment to identify sediment sources. The *n*-alkanes were based on land uses, could provide vegetation information, and were relatively resistant to diagenetic modifications and decomposition. This study used a composite fingerprinting method that was based on two types of fingerprint factors (27 biomarker properties and 45 geochemical properties) with 60 source samples (i.e., gully, grassland, forest, and cropland) and nine soil profiles. Genetic algorithm (GA) optimization has been deployed to find the optimal source contribution to sediments. The biomarker results demonstrated that young forest is the main sediment source in this catchment, contributing 50.5%, whereas cropland, grassland and gully contributed 25.6%, 14.4% and 9.5%, respectively; the geochemistry results were similar to the biomarkers. The forest and grassland contributions gradually increased from upstream to downstream, and the sediment contributions of cropland gradually decreased in the direction of the runoff pathway at the check dam. In a comparison of biomarker and geochemical fingerprinting data, the latter may have overestimated the forest inputs to the catchment sediment yields because of a mixed land use history (i.e., forest and grassland). The geochemical fingerprint approach limits its ability to fully discriminate sources based on land management regimes, but the biomarker (individual *n*-alkanes)

* Corresponding author at: State Key Laboratory of Soil Erosion and Dryland Farming on the Loess Plateau, Northwest A & F University, Yangling 712100, PR China.
E-mail addresses: chenfx_520@163.com (F. Chen), fnf@ms.iswc.ac.cn (N. Fang), shizhihua70@gmail.com (Z. Shi).

displayed the potential to discriminate between a greater number and different types of sediment sources and to provide greater detail regarding sediment sources.

1. Introduction

Information regarding sediment sources has considerably enhanced our understanding of sediment provenance and the development of catchment sediment budgets (Walling, 2005). Sediment redistribution exerts significant control on the transport and fate of nutrients, organic and inorganic contaminants, and trace or heavy metals (Collins et al., 2010, 2012a; Haddadchi et al., 2013; Zhang et al., 2013). In response to these sediment-related environmental problems, reliable information on sediment sources is critical if mitigation measures are to be targeted effectively. The sediment fingerprinting method has provided a direct and successful approach to quantify sources of sediment from individual river sections to a catchment scale over the previous 30 years (Collins et al., 1997; Walling, 2005; Davis and Fox, 2009; Collins et al., 2010, 2012a, 2012b).

Because of the distinct geophysical and geochemical properties of sediment sources, sediment fingerprinting can help determine the proportion of suspended sediment in a waterway that originates from a specific source within a catchment (Haddadchi et al., 2013; Koiter et al., 2013). Traditional fingerprinting factors have included geochemical factors (Collins et al., 2012a), environmental magnetism (Rotman et al., 2008), rare earth elements (REEs) (Kimoto et al., 2006), radionuclides (Wallbrink et al., 1998), particle shapes (Hatfield and Maher, 2009), and color properties (Martínez-Carreras et al., 2010a, 2010b). However, traditional tracers cannot always distinguish erosion sources by land use when the geologic variations within a study area are small or when different land uses span geological boundaries (Gibbs, 2008; Hancock and Revill, 2013). Current geochemical and geophysical approaches cannot provide vegetation information regarding sediment sources, which represents a major shortcoming of previous research (Blake et al., 2012). Erosion processes are not always related to catchment geology (Hancock and Revill, 2013). Previous studies have indicated that land use is one of the most important factors that directly influence soil erosion (Fang et al., 2012). If new fingerprint properties could improve the relationship between different land use and sediment yield, fingerprinting methods would become more comprehensive.

In particular, n-alkane biomarkers provide a potential fingerprinting source. Previous studies have shown that various types of plants produce leaf waxes (n-alkanes) with various carbon chain lengths. Long-chain n-alkanes (C_{27}–C_{35}) with a strong odd/even predominance are a main component of the epicuticular wax of higher plants (Silva et al., 2012). C_{31} or C_{33} n-alkanes dominate in most grasses and herbs, whereas C_{27} or C_{29} n-alkanes dominate in most trees and shrubs (Zech et al., 2013). Aquatic algae and microbes are dominated by shorter-chain n-alkanes (C_{15}–C_{19}; Meyers (2003)), whereas middle-chain n-alkanes (C_{20}–C_{25}) are a dominant component of submerged aquatic macrophytes (Ficken et al., 2000). These plant communities would naturally label the soil and environment where they grow by exuding organic biomarkers because of the leaf waxes and associated n-alkanes are not especially water-soluble (Gibbs, 2008; Guzmán et al., 2013). Hydrocarbon molecules are more resistant to diagenetic modifications and decomposition than other forms of organic matter, such as carbohydrates, fatty acids, amino acids and lignin (Matsumoto et al., 2007; Cooper et al., 2015). The former provide long-lived indications of changes in sources of organic matter to a catchment (Meyers, 2003). Based on these theories, the individual n-alkanes may discriminate between land uses within a given geologic region.

The loess hilly-gully regions in northwestern China were transported by fierce wind storms during the Quaternary period, and the soil and geologic conditions are generally homogeneous (Tsunekawa et al., 2014). However, the land use/cover in a small catchment usually includes several different landscapes, e.g., forest, grassland, and cropland. In 1999, the Chinese central government initiated a nationwide cropland set-aside program that is known as the Grain-for-Green Project (Fu et al., 2006). The Grain-for-Green Project was developed to increase forest and grassland cover. As a part of this project, vast areas of cropland with a slope gradient that exceeded 25° in mountainous areas were converted to forestland or grassland in the gully and hilly zones of the Loess Plateau. For cropland with other slopes, governments designate a certain quota of cropland in each province every year, and farmers who agree to stop cultivating these lands receive subsidies to cover their loss. Thanks to this income, these farmers will not convert forest or grassland to cropland in the usual manner. The landscape structure has become more stable following the Grain-for-Green Project. Constructing check dams in gullies has been the most widespread and effective strategy to reduce soil and water loss (Shi and Shao, 2000; Wang et al., 2014). Check dams trap all of the sediment that is derived from upstream soil erosion, and the sediment in check dams has a well-documented history of soil erosion. Stable landscapes and sediments that are trapped by check dams provide a source of biomarkers that can be used to identify sediment sources. In the organic geochemistry, n-alkanes were the most widely biomarkers, which were used to track the sources of organic matters (Meyers, 2003). However, few studies focused on using the individual n-alkanes to identify sediment sources directly, only some researches based on the compound-specific isotope analysis (CSIA) of biomarkers to track sediment sources (Gibbs, 2008; Blake et al., 2012; Hancock and Revill, 2013; Cooper et al., 2015). The latter is often restricted to the instrument, measurement of the individual n-alkanes only needs a gas chromatograph fitted with a flame ionization detector (GC-FID), but the CSIA requires to use the isotope ratio mass spectrometer (IRMS) coupled with a GC–Isolink gas chromatograph (GC–IRMS). Guzmán et al. (2013) indicated that the fingerprinting research for the future is the development of tracers requiring inexpensive and rapid analysis approaches that are able to process quickly a large number of samples. It indicated that the individual n-alkanes technique was more convenient than CSIA. This paper describes work that was designed to assess the ability of the biomarker fingerprinting technique to discriminate eroded soil sources in a small catchment of the Loess Plateau in northwestern China.

2. Materials and methods

2.1. Study area

The Hujiawan catchment is located in the middle portion of the Loess Plateau between 36.4°N and 36.6°N latitude and between 109.5°E and 109.9°E longitude and covers an area of 27 km² (Fig. 1). The elevations within the catchment range from 947 m to 1300 m, and the slope gradient ranges from 0 to 55.3°, with an average of 14.2°; areas where the gradients exceed 10° constitute 75.1% of this catchment (Fig. 2). This region is characterized by a semiarid climate, and the annual precipitation averages 497 mm. Precipitation is mainly concentrated during the rainy season (i.e., from June to September), representing 60–70% of the annual total, most of which occurs in the form of high-intensity rainstorms (Yang et al., 2006). The soil in this region has primarily developed from loess parent materials and has a silty loam texture. The loess layers in the middle Loess Plateau generally have thicknesses of 80–120 m (300–400 m in typical highland areas) and are the thickest known loess deposits in the world, being much thicker than those in Europe and the Americas (Liu, 1985). This
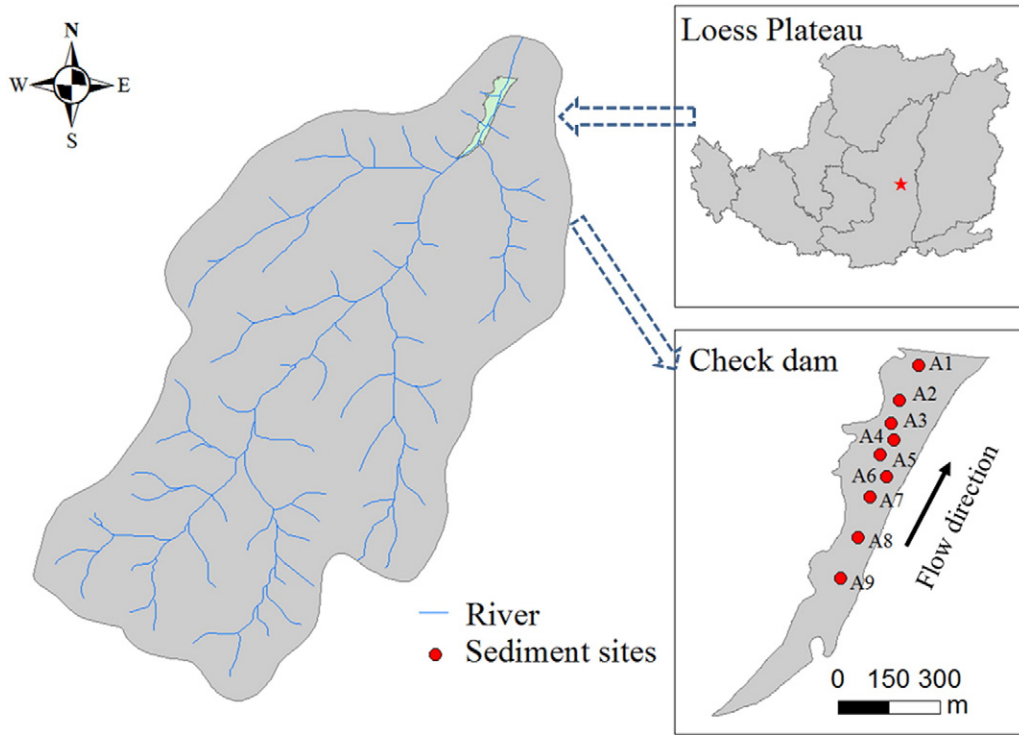
Fig. 1. Location of the study area and sediment sampling sites.

homogenous soil has a texture that ranges from fine silts to silt and is vulnerable to erosion (Fu et al., 2000).

A catchment topographic map (scale 1:10,000) was used in land-use classification alongside 2010 QuickBird imagery. Reconnaissance field surveys were conducted in May 2014, and all the images that are used in this study were captured during that period; the land-use history was reconstructed based on interviews with local villagers. Land use units were delineated on the photographs and verified in the field, as

Land use	Proportion (%)
Forest	63.3
Grassland	26.7
Cropland	6.7
Residential area	3.7
Check dam	0.6

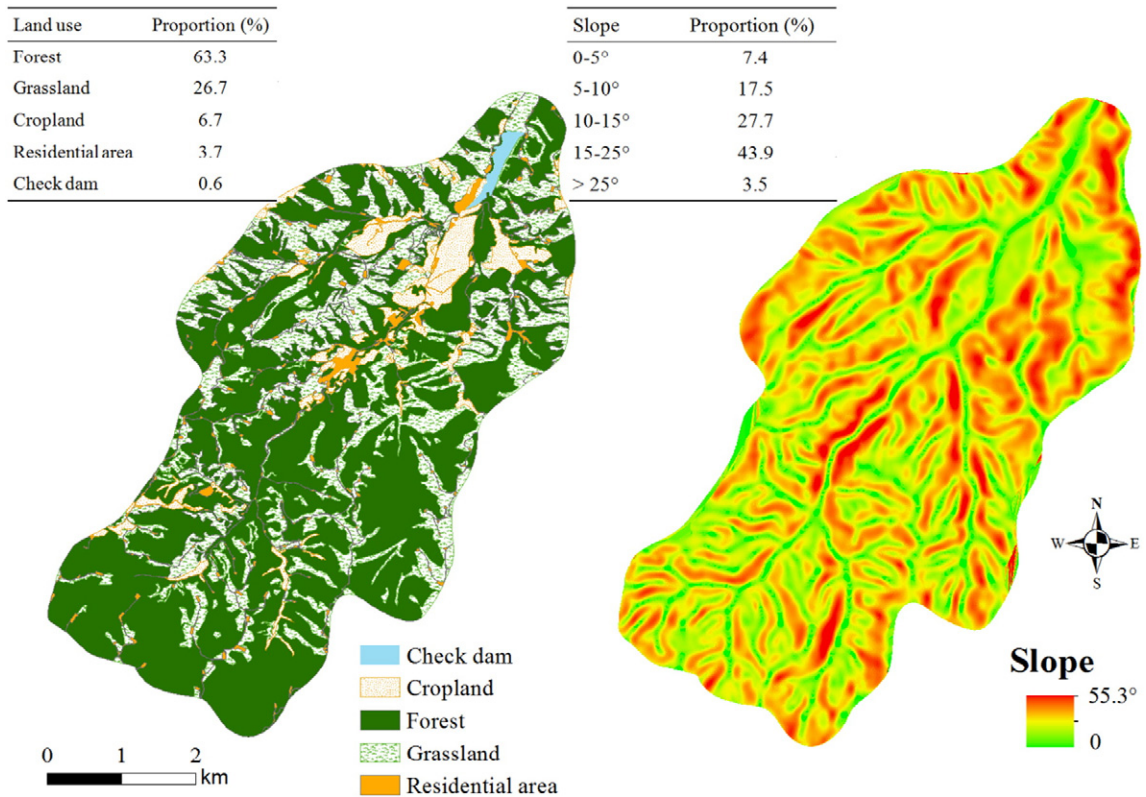| Slope	Proportion (%)
0-5°	7.4
5-10°	17.5
10-15°	27.7
15-25°	43.9
> 25°	3.5

Fig. 2. Land use/cover and slope gradients of the study catchment.

shown in Fig. 2. In this catchment, the primary land use is forest. Only a few of the original forests remain, and many of the original forests were gradually converted into cropland under the Household Contract Responsibility System (Tsunekawa et al., 2014). However, this condition was changed with the Grain-for-Green Project in 1999; vast areas of cropland were converted to forest over the previous 15 years (Fu et al., 2006). The species composition of the young forests is relatively simple (*Robinia pseudoacacia*), the leaf litter is poorly developed, and the young forests tend to have exposed soil surfaces. Forest covers 62.3% of the study area, grassland 26.7%, and cropland only 6.7%. The majority of the forests are located in steep areas, whereas croplands are located in relatively level areas (Fig. 2).

2.2. Soil samples

The fieldwork involved the collection of representative samples of source materials and the sediment deposit profiles that drain the Hujiawan catchment. In this catchment, natural fallow land hardly contributes sediments (Chen et al., 2016). Source material sampling involved the collection of 60 samples of surface soil from eroding areas that represent each of the uncultivated (grassland, forest, gully) and cultivated (cropland) sites: 15 samples from gully, 15 from grassland, 15 from young forests, and 15 from cropland. For each source sample, 10 sub-samples were collected from 0 to 5 cm depth along transects at a 5×5 m grid and combined in the field to form a single composite sample. Sediment sampling was performed from head to tail along the check dam silted plane. We dug nine sediment profiles in the check dam (Fig. 1) and carefully sectioned the profiles to reflect the flood couplets. The sediments were undisturbed, as indicated by the clear water-sediment interface and the preservation of fine sediment laminations. The boundary between the couplets that were associated with individual floods was easily defined because the bottom layer in each couplet was coarse, whereas the top was fine (Wang et al., 2014). In the fieldwork, almost each flood couplet was composed of one layer of clay and one layer of sand; this structure made it easier to distinguish each flood couplet. The thickness of each couplet varied from a few centimeters to several decimeters. We collected three flood couplet samples from each sediment profile (A1, A2, A3, A4, A5, A6, A7, A8, and A9).

2.3. Laboratory analysis

Concentrations of total organic carbon (TOC) were determined by using the oil bath-$K_2Cr_2O_7$ titration method. We analyzed soil samples with the laser diffraction technique using a laser particle size analyzer (Mastersizer 2000, England); the measurements spanned sizes from 0.02 to 2000 μm. The geochemical properties of the samples were analyzed by using ICP-MS; a total of 45 potential fingerprint properties were measured (i.e., Mo, Cu, Pb, Zn, Ag, Ni, Co, Mn, Fe, As, U, Th, Sr, Cd, Sb, Bi, V, Ca, P, La, Cr, Mg, Ba, Ti, Al, Na, K, W, Zr, Ce, Sn, Y, Nb, Ta, Be, Sc, Li, S, Rb, Hf, In, Re, Se, Te, and Tl). Sample analysis and quality assurance were performed by Acme Labs (Vancouver Office, Canada).

The total lipids were extracted from powdered soil samples by ultrasonication and were centrifuged by using a solvent system with a 9:1 solution of MeOH/CH_2Cl_2. Each sample was dipped for 6 h and extracted ultrasonically for 15 min each time. The extracts were combined and concentrated under a stream of nitrogen, saponified by adding two ml of 6% KOH in MeOH and then held for 12 h. The non-saponifiable lipids were isolated by hexane extraction four times and concentrated by solvent evaporation under a N_2 gas stream. After saponification, the clean-up and separation of extracts were accomplished by passing samples through a chromatographic column (20 cm × 10 mm) of activated silica (24 h at 120 °C, then deactivated with 5% H_2O). The nonpolar fraction (*n*-alkanes) was measured using a gas chromatograph (GC) (Agilent 7890 A, USA) equipped with a DB-5MS (Agilent, USA), capillary column (30 m × 0.25 mm × 0.25 μm), and flame ionization detector (FID). Both

the injector and detector were set at 300 °C. Nitrogen was used as the carrier gas with a flow rate of 1.2 ml/min by split-less injection. The temperature program for the oven was as follows: heating from 80 °C to 15 °C at 10 °C min^{-1}, ramping from 160 °C to 300 °C at 6 °C min^{-1}, and finally holding at 300 °C for 10 min; the total run time was 42 min. Hexatriacontane (C_{36}) was added as an internal standard, and a set of *n*-alkanes C_8–C_{40} (Accustandard) from *the o2si smart solutions* (USA) was used as the reference material. The components were analyzed daily by using the same GC measuring devices and procedures. Blank samples were analyzed by following the exact same procedure. The results indicated no UCM (unresolved complex mixture) or detectable peaks for the *n*-alkane distributions that were discussed here, thereby implying that no contamination occurred during our sample preparation.

Absolute concentrations of *n*-alkanes have not yet successfully detected the origin of organic matter. To determine the likely sources more precisely, various hydrocarbon indices, in addition to the absolute concentrations, were analyzed. The abbreviations for the hydrocarbon indices are shown in Table 1.

2.4. Sediment fingerprinting procedure

The non-conservative behavior of sediment properties has significant implications for the sediment fingerprinting technique (Koiter et al., 2013). According to the research of Wilkinson et al. (2013), tracers were selected for inclusion in source fingerprints based on compliance with three constraints. First, conservative behavior during erosion and transport was assured by all sediment sample concentrations that fell within the observed range of soil source samples, and the sediment mix's mean concentration for each tracer was within the range of the source soil's mean concentrations. Second, the coefficient variation (CV) of the sediment samples was inherently smaller than that of the sources, which enabled some tracers to satisfy the first constraint despite having mean concentrations that were close to those of the outlying source samples. Third, the power of individual properties to discriminate between sources was tested by using the Kruskal-Wallis rank sum test, and properties that returned a *P*-value >0.05 were excluded. Then, a stepwise Discriminant Function Analysis (DFA) was used to further assess the discriminatory power of those tracer properties that passed the three constraints. DFA identifies an optimal source fingerprint that comprises the minimum number of tracer properties that provide the greatest discrimination between the analyzed source materials based on the minimization of Wilks' lambda. The lambda value approaches zero as the variability within the source categories is reduced relative to the variability between categories based on the entry or removal of tracer properties from the analysis. The results of the DFA were used to examine the proportion of samples that were accurately classified into the correct source groups.

Table 1
Hydrocarbon indices and their abbreviations in this research.

Hydrocarbon indices	Abbreviations	Reference
Carbon preference index	CPI	Meyers (2003), Zheng et al. (2007)
Odd-over-even predominance	OEP_M OEP_L	Kolattukudy et al. (1976), Rogers et al. (1999), Zech et al. (2012)
Average chain length	ACL	Cranwell (1973), Meyers (2003)
$(C_{23} + C_{25})/(C_{23} + C_{25} + C_{29} + C_{31})$	P_{aq}	Ficken et al. (2000)
$(C_{27} + C_{29} + C_{31})/(C_{23} + C_{25} + C_{27} + C_{29} + C_{31})$	P_{wax}	Zheng et al. (2007)
$C_{31}/(C_{27} + C_{29})$	HVI	Tareq et al. (2005)
C_{31}/C_{27}	–	Brincat et al. (2000)
C_{31}/C_{29}	–	Hu et al. (2003)

OEP_M: odd-over-even predominance of the middle chain *n*-alkane patterns (C_{20}–C_{25}).
OEP_L: odd-over-even predominance of the long chain *n*-alkane patterns (C_{26}–C_{33}).

The multivariate mixing model is based on a set of linear equations. In this model, each selected tracer property is represented by an equation that relates the tracer concentration in a sediment sample to the sum of the mean tracer concentrations in each source multiplied by the respective unknown proportional source contributions. Solutions to the mixing model are obtained by using an optimization procedure that selects values of P_s that minimize the sum of the squares of the relative errors in the objective function, as shown in Eq. (1);

$$f = \sum_{i=1}^{n} \left\{ \left(1 - \frac{\left(\sum_{s=1}^{m} P_s S_{si} Z_s O_s \right)}{C_i} \right) \right\}^2 W_i \tag{1}$$

where f is the minimum of the sum of the squares of the relative errors, C_i is the concentration of each fingerprint property (i) in the sediment that was collected from the check dam, P_s is the optimized percentage contribution from source category (s), S_{si} is the mean concentration of the fingerprint property (i) in the source category (s), Z_s is the particle size correction factor for the source category (s), O_s is the organic matter content correction factor for the source category (s), W_i is the tracer-specific weighting that reflects the analytical precision, n is the number of fingerprint properties that comprise the optimal composite fingerprint, and m is the number of sediment source categories (Collins et al., 1997).

The model is constrained by the requirements that proportional source contributions lay between 0 and 1 and that the proportional source contributions sum to 1. The tracer-specific weighting was included so the tracer properties with the least variance exerted greater influence on the mixing model solutions. This weighting was calculated as the inverse of the square root of the variance of tracer data for each source that had been standardized based on the respective source means (Collins et al., 1997).

Genetic algorithm (GA) optimization (population size = 50, cross over ratio = 0.5, mutation rate = 0.1; Haddadchi et al. (2013)) has been deployed to find the optimal source contribution to sediments. In this study, the mean relative contribution from each source, which used 5000 iterations of Monte Carlo techniques as a surrogate of conventional random sampling, and genetic algorithm optimization were used to predict more accurate source contributions. As in other hydrological modeling, the uncertainty issues that are associated with the results of sediment source fingerprinting studies have attracted increasing attention in recent years (Collins et al., 2012a; Walling, 2013). Important sources of uncertainty include the mixing model optimization and the property values that are used to characterize both sources and targets. Source characterization, in particular, can involve many uncertainties because soil properties are likely to vary spatially and may vary in response to the intensity of erosion (Walling, 2013). The representation of a given source by a series of single property values, as required by a standard mixing model, may therefore be unrealistic. Sediment source fingerprinting studies are increasingly considering the inherent variability of the properties of given sources by incorporating Monte Carlo techniques into mixing model optimization routines to represent the uncertainty that is associated with source characterization and to propagate this uncertainty to the final source ascription results. Usually, the mean or median of the values for individual properties that are obtained for the samples that were collected to represent a given source is used, and its standard error should be considered (Walling, 2013); the final result of the source ascription exercise can then be represented as a range of values and confidence limits (95%) (Franz et al., 2014).

The goodness of fit (GOF) that was provided by the optimized mixing model was assessed by comparing the actual fingerprint property concentrations in the sediment samples with the corresponding values that were predicted by the mixing model based on the estimates of the magnitude of the contributions from each of the sources (Walling, 2005). A GOF estimator (Collins et al., 2010) was used to examine the efficiency of the model to predict the measured biomarker and

geochemistry for the sediment samples that were collected at the outlet of the Hujiawan catchment.

3. Results and discussion

3.1. Potential fingerprint properties

In most of the samples, the n-alkane distributions ranged from C_{18} to C_{35}. A few samples contained no detectable levels of C_{34} and C_{35}, including seven grassland samples, five forest samples and two cropland samples. For the biomarker, a total of 27 potential fingerprint properties, including n-alkanes and hydrocarbon indices (i.e., C_{18}, C_{19}, C_{20}, C_{21}, C_{22}, C_{23}, C_{24}, C_{25}, C_{26}, C_{27}, C_{28}, C_{29}, C_{30}, C_{31}, C_{32}, C_{33}, C_{34}, C_{35}, CPI, OEP$_M$, OEP$_L$, ACL, P$_{aq}$, P$_{wax}$, HVI, C_{31}/C_{27}, and C_{31}/C_{29}) were measured, as shown in Table 2. The observed distributions of n-alkanes clearly showed a higher abundance of middle-chain components in the source samples. Fig. 3 shows the relative intensity of the average concentrations of four land-uses: in all sources, the middle-chain n-alkanes (C_{20}–C_{25}) accounted for large proportions and had no significant odd-over-even predominance, whereas long-chain n-alkanes (C_{27}–C_{35}) had a significant odd-over-even predominance, except for the gully samples. The maximum peak of the homologues appeared in the long-chain components (C_{29}, Fig. 3c) in the forest samples, whereas the maximum peak of the other sources appeared in the middle-chain components (C_{23} (cropland), C_{24} (gully), C_{25} (grassland); Fig. 3d, a, and b).

Zech et al. (2012) used the odd-over-even predominance of the middle chain n-alkane patterns (OEP$_M$) and the long chain n-alkane patterns (OEP$_L$) to expression the degree of degradation. The middle chain component (C_{20}–C_{25}) had no significant odd-over-even predominance (OEP$_M$) (Fig. 3). However, the long chain component (C_{27}–C_{35}) had significant odd-over-even predominance (OEP$_L$) in grassland, forest,

Table 2
Biomarker soil source tracers that passed (P) each constraint for input to the fingerprint optimization procedure.

Tracers	Unit	Mean	Min	Max	Sediment mean inside[a]	Sediment samples inside[b]	H-value	P-value
C_{18}	ppm	0.8	0.1	1.8	P			
C_{19}	ppm	2.7	0.9	6.8	P			
C_{20}	ppm	2.3	0.6	4.6	P	P	14.607	0.002*
C_{21}	ppm	5.1	2.4	11.9	P	P	9.822	0.020*
C_{22}	ppm	6.5	3.5	14.9	P	P	20.225	0.000*
C_{23}	ppm	11.2	6.2	22.3	P	P	20.088	0.00*0
C_{24}	ppm	13.5	5.4	34.2	P	P	24.608	0.000*
C_{25}	ppm	14.5	5.5	41.7	P	P	25.272	0.000*
C_{26}	ppm	11.4	3.2	33.2	P	P	28.584	0.000*
C_{27}	ppm	11.1	4.3	26.5	P	P	19.888	0.000*
C_{28}	ppm	6.0	0.8	17.4	P	P	29.875	0.000*
C_{29}	ppm	9.6	2.8	33.4	P	P	14.223	0.003*
C_{30}	ppm	3.2	0.7	11.3	P	P	21.055	0.000*
C_{31}	ppm	7.2	1.8	24.4	P	P	5.178	0.159
C_{32}	ppm	1.5	0.5	6.1	P	P	17.166	0.001*
C_{33}	ppm	2.7	0.7	10.6	P	P	5.083	0.166
C_{34}	ppm	–	–	2.1				
C_{35}	ppm	–	–	3.6				
CPI		1.4	1.2	5.4	P	P	46.484	0.000*
OEP$_M$		1.6	1.2	1.7	P	P	24.212	0.000*
OEP$_L$		2.4	0.8	4.1	P	P	40.439	0.000*
ACL		29.3	28.3	30.3	P	P	13.355	0.004*
P$_{aq}$		0.7	0.3	0.8	P	P	15.004	0.002*
P$_{wax}$		0.8	0.3	0.8	P	P	13.110	0.004*
HVI		0.7	0.3	1.8	P	P	17.777	0.000*
C_{31}/C_{27}		0.3	0.4	1.5	P	P	3.501	0.478
C_{31}/C_{29}		0.3	0.2	2.9	P	P	4.182	0.382

* Significant at $P < 0.05$, ppm is parts per million, "–" means that the tracers were not detected in some source samples.
[a] Mean sediment concentration within the range of the source category mean values.
[b] All sediment sample concentrations were within the range of the source sample values; in this example, constraints 1 and 2 were applied by using sediment from the Hujiawan catchment.
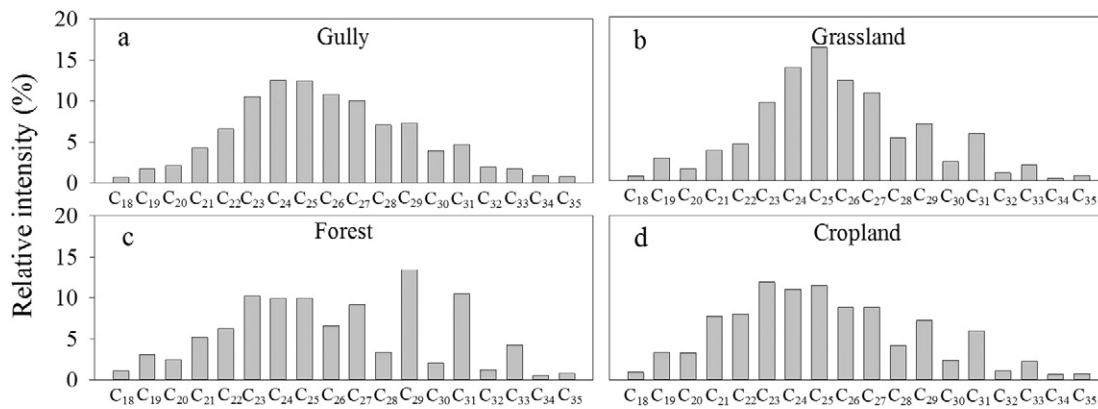
Fig. 3. The *n*-alkane distributions of the samples.

and cropland. For the high concentrations of C_{23} and C_{25} alkanes, the previous explanation was derived from the aquatic organic matter inputs (Fang et al., 2014), based on this theory, scholars used P_{aq} of the lake or ocean sediments to calculate aquatic and terrestrial plants proportions (Ficken et al., 2000). However, the water in check dam would discharge through the spillway; the check dam could not provide a suitable environment for the aquatic macrophytes. For the long chain *n*-alkanes, the hydrocarbons showed a unimodal distribution with concentration maxima corresponding to the odd carbon-number compounds in the range of C_{27}–C_{35}, and this distribution pattern has been used extensively as an indicator of prominent terrigenous input derived from higher plant waxes (Ho and Meyers, 1994; Zhao et al., 2003; Fang et al., 2014). Meyers and Ishiwatari (1993) indicated that hydrocarbon molecules were relatively more resistant to diagenetic modifications than other forms of organic matter. It may lead to a low concentration of organic matters but a relative high concentration of hydrocarbons in the parent material of loess, e.g., the soils in gully. Therefore, the high proportions of middle-chain *n*-alkanes may have been derived from paleosol-loess. Meanwhile, the paleosol-loess may dilute the long chain *n*-alkanes which derived from higher plant waxes. It caused the special distributions of *n*-alkanes in source soils, which the middle chain *n*-alkanes accounted for a very large proportion, as shown in Fig. 3.

The carbon preference index (CPI) and average chain length (ACL) of the four land-use types could support sources of the middle chain *n*-alkanes. In organic geochemistry, previous studies have used ACL and CPI to differentiate organic material of higher plant origin from algal or microbial contributions, or to identify petrogenic hydrocarbon inputs (Tareq et al., 2005; Jeng, 2006). The CPI for the four land-use types varied from 1.2 to 5.4 with an average of 1.4, and the forest had the max average value (4.0), followed by cropland (2.3), grassland (2.1) and gully (1.4), respectively. Low CPI values in gully indicated contributions from ancient organic matters weathered out of the soil profile, and higher CPI indicated organic matters derived from higher plant inputs (Pancost and Boot, 2004). This ancient material may reflect relic plant communities that bear little resemblance to the modern intensive arable system (Cooper et al., 2015). The ACL for the four land-use types varied from 28.3 to 30.3 with an average of 29.3, and the forest had the largest ACL, followed by cropland, grassland and gully, respectively. In the most of sediment samples, the maximum peak of the homologues appeared in the long-chain components (C_{29} (12 times) and C_{31} (7 times)), several samples appeared in the middle-chain components (C_{24} (2 times) and C_{25} (6 times)), and the average distribution of the *n*-alkanes in sediments was similar to the distribution of forest. If identifying the sources of sediments only from the perspective of the *n*-alkanes distribution, the forest may be a major source of sediments in this catchment.

In addition, both in the source and sediment samples, a total of 42 potential geochemical fingerprint properties (three elements was not detected in the samples, namely, S, Re, and Se), were measured, as shown in Table 3.

3.2. Sediment source discrimination

A total of 25 biomarker trackers (C_{34} and C_{35} were not detected in some source soils) passed the constraint that the mean of the sediment sample concentrations was within the range of the source mean concentrations. Of these elements, 23 biomarker trackers (i.e., C_{20}, C_{21}, C_{22}, C_{23}, C_{24}, C_{25}, C_{26}, C_{27}, C_{28}, C_{29}, C_{30}, C_{31}, C_{32}, C_{33}, CPI, OEP_M, OEP_L, ACL, P_{aq}, P_{wax}, HVI, C_{31}/C_{27}, and C_{31}/C_{29}) had all sediment samples within the range of source values, with exceptions generally being those that were associated with surface mixing. Nineteen properties (i.e., C_{20}, C_{21}, C_{22}, C_{23}, C_{24}, C_{25}, C_{26}, C_{27}, C_{28}, C_{29}, C_{30}, C_{32}, CPI, OEP_M, OEP_L, ACL, P_{aq}, P_{wax}, and HVI) returned P-values <0.05 from the Kruskal-Wallis H test; the H-value ranged from 9.822 to 46.484, as shown in Table 2. The short-chain *n*-alkanes (C_{18} and C_{19}) did not pass constraints 1 and 2 because the concentrations in the sediments were beyond the range of the sources (Table 2). Biological activity mainly affected the short-chain content (C_{15}–C_{19}) in two ways. First, the activities of algae and photosynthetic bacteria (e.g., blue algae or blue-green algae, Han et al., (1968)) in sediments would increase with the short-chain content (C_{15}–C_{19}) (Gelpi et al., 1970; Meyers and Ishiwatari, 1993; Meyers, 2003). Second, the lower-molecular-weight *n*-alkanes (C_{15}–C_{19}) that typify algae are generally more susceptible to microbial degradation than land-plant *n*-alkanes (Meyers, 2003; Matsumoto et al., 2007). The middle and long chain *n*-alkanes passed the two constraints (Table 2) because the microbes may have less influence in the middle and long chain *n*-alkanes (Meyers, 2003), and no additional inputs from aquatic macrophytes in this water-deficit environment.

For the geochemical trackers, all 42 elements passed the constraint that the mean sediment sample concentration was within the range of the source mean concentrations. Thirty-one elements (i.e., Mo, Pb, Ag, Mn, As, U, Th, Sr, Cd, Sb, Ca, P, La, Cr, Mg, Ba, Ti, K, W, Zr, Sn, Y, Nb, Ta, Be, Sc, Rb, Hf, In, Te and Tl) passed the constraint that all of the sediment samples were within the range of the source values. These constraints excluded elements likely to be soluble or significantly associated with organic matter (Wilkinson et al., 2013). A total of 17 properties returned a P-value <0.05 from the Kruskal-Wallis H test, and the H-value ranged from 7.916 to 35.553. Finally, 17 geochemical trackers (i.e., Mo, Pb, U, Sr, Cd, Sb, Ca, P, La, Cr, Mg, Ti, Zr, Y, Ta, Sc, and Tl) passed the three constraints, as shown in Table 3.

The tracers passed the three constraints and consequently underwent a stepwise discriminant function analysis (DFA). In this case, the optimal composite fingerprint consisted of a total of six biomarker properties (i.e., CPI, OEP_M, C_{28}, C_{21}, C_{24}, and C_{26}) and correctly distinguished 86.7% of the samples that were used to characterize

Table 3
Geochemical soil source tracers that passed (P) each constraint for input to the fingerprint optimization procedure.

Element	Unit	Mean	Min	Max	Sediment mean inside[a]	Sediment samples inside[b]	H-value	P-value
Mo	ppm	0.7	0.4	1.6	P	P	20.619	0.000*
Cu	ppm	22.5	19	31.2	P			
Pb	ppm	22.5	19	33.1	P	P	7.916	0.048*
Zn	ppm	64.8	53	103	P			
Ag	ppm	0.1	0.1	0.1	P	P	0.000	1.000
Ni	ppm	31.6	25.7	43.2	P			
Co	ppm	12.3	10.5	15.6	P			
Mn	ppm	631.7	454	833	P	P	6.459	0.091
Fe	%	3.0	2.47	3.73	P			
As	ppm	13.3	10	17	P	P	6.450	0.092
U	ppm	2.3	1.5	3.3	P	P	15.026	0.002*
Th	ppm	12.3	8.9	15.3	P	P	3.740	0.291
Sr	ppm	219.7	143	264	P	P	15.040	0.002*
Cd	ppm	0.2	0.1	0.4	P	P	10.116	0.018*
Sb	ppm	1.6	1.2	2	P	P	12.838	0.005*
Bi	ppm	0.4	0.3	0.5	P			
V	ppm	75.2	62	99	P			
Ca	%	4.7	2.52	6.3	P	P	8.276	0.041*
P	%	0.1	0.042	0.083	P	P	20.897	0.000*
La	ppm	34.4	24.8	39.1	P	P	13.367	0.004*
Cr	ppm	53.8	40	73	P	P	13.689	0.003*
Mg	%	1.3	1.01	1.59	P	P	35.553	0.000*
Ba	ppm	464.1	395	550	P	P	1.949	0.583
Ti	%	0.4	0.301	0.441	P	P	27.093	0.000*
Al	%	5.9	5.4	6.91	P			
Na	%	1.2	0.492	1.395	P			
K	%	1.9	1.78	2.38	P	P	4.375	0.224
W	ppm	1.7	1.4	2	P	P	2.150	0.542
Zr	ppm	68.8	56.6	91.2	P	P	13.376	0.004*
Ce	ppm	66.1	49	72	P		5.629	0.131
Sn	ppm	2.6	2.1	3.5	P	P	6.640	0.084
Y	ppm	19.6	16.3	23.4	P	P	21.462	0.000*
Nb	ppm	10.2	8.8	12.3	P	P	2.273	0.518
Ta	ppm	0.8	0.7	0.9	P	P	8.133	0.043*
Be	ppm	1.8	1	3	P	P	1.445	0.695
Sc	ppm	10.2	9	12	P	P	15.070	0.002*
Li	ppm	34.0	28.3	41.3	P			
S	%	–	–	–				
Rb	ppm	90.5	73.7	104.3	P	P	6.142	0.105
Hf	ppm	2.0	1.6	2.7	P	P	3.616	0.306
In	ppm	0.1	0.05	0.08	P	P	5.767	0.124
Re	ppm	–	–	–				
Se	ppm	–	–	–				
Te	ppm	0.8	0.5	1.1	P	P	4.149	0.249
Tl	ppm	0.5	0.5	1	P	P	10.493	0.015*

* Significant at $P < 0.05$, ppm is parts per million, units are weights in % (Fe, Ca, P, Mg, Ti, Al, Na, K, and S), "–" means that the tracers were not detected in some source samples.
[a] Mean sediment concentration within the range of the source category mean values.
[b] All sediment sample concentrations were within the range of the source sample values; in this example, constraints 1 and 2 were applied by using sediment from the Hujiawan catchment.

Table 4
Optimal composite fingerprints for discriminating individual sediment source types in the Hujiawan catchment.

Geochemistry				Biomarker			
Step	Tracer property	Wilks' lambda	Cumulative classified correctly (%)	Step	Tracer property	Wilks' lambda	Cumulative classified correctly (%)
1	Mg	0.296	51.7	1	CPI	0.228	66.7
2	Ti	0.200	68.3	2	OEP_M	0.126	81.7
3	Sc	0.121	78.3	3	C_{28}	0.086	86.7
4	Pb	0.084	83.3	4	C_{21}	0.069	86.7
5	U	0.062	80.0	5	C_{24}	0.055	80.0
6	Y	0.046	91.7	6	C_{26}	0.041	86.7
7	Zr	0.036	90.0				

small percentage of the bulk organic matters (Meyers, 1997), soil lipids constitute between 4 and 8% soil organic carbon, but quantities of 42% have been observed in cultivated organic soil (Bull et al., 2000). In addition, because a relative high concentration of middle chain n-alkanes remained in soil of gully, the gully also has high classification accuracy.

3.3. Sediment source apportionment

The 95% confidence limits around the predicted average median source type proportions, which were generated by using the repeat sets, clearly indicated the convergence of the model solutions and their reproducibility within ± 3%. Meanwhile, the mean values of the repeat sets represented the sediment contribution of a given source. According to Walling (2005), the mixing model algorithm can provide an acceptable prediction of the fingerprint property concentrations that are associated with the sediment samples from the study catchment. For the biomarkers, the GOF of all the samples ranged from 87.1% to 99.0%, with an average of 95.4% ± 3.6%; for the geochemical properties, the GOF of all the samples ranged from 93.4% to 99.4%, with an average of 97.8% ± 1.5%. The results of biomarker and geochemical indicated that the relative contributions from the individual source types generated by the mixing model were meaningful, with a GOF criterion of >80.0% (McKinley et al., 2013).

The nine soil profiles were distributed along the check dam from upstream (core A9) to downstream (core A1). Fig. 4 summarizes the source ascription results from the nine sediment profiles that were collected from the check dam. The substantial variability in the contributions from the four sources to the individual samples is a key feature of the results. The calculated mean relative contribution of each source type to the sediment from the biomarkers indicated that the primary sources are forests, which contributed 50.5%, whereas cropland, gully and grassland contributed 25.6%, 9.5%, and 14.4%, respectively. Compared to biomarkers, the geochemical property results were similar in gully and cropland, which contributed 10.4% and 23.9%, whereas grassland and forests contributed 8.0% and 57.7%, respectively. Both results indicated that the relative contribution of each source type varied from one location to the next near the check dam because of variations in hydrodynamic conditions (Wang et al., 2014). For the biomarkers, the forest and grassland contributions gradually increased from upstream (sites A7, A8, and A9) to downstream (sites A1, A2, and A3; Figs. 1 and 5), and the sediment contributions of cropland gradually decreased in the direction of the runoff pathway. In the midstream portion (sites A4, A5, and A6), the gully contribution was greater than those of the upstream (sites A7, A8, and A9) and downstream portions (sites A1, A2, and A3). However, the geochemical property results indicated that only the sediment contributions of gully gradually decreased in the direction of the runoff pathway, and the maximum contributions of the other sources occurred in different portions of check dam, specifically, grassland in the midstream section, forests in the upstream section and cropland in the downstream section. Three flood couplets represented three erosive rainfall events in this catchment, the vertical variation of
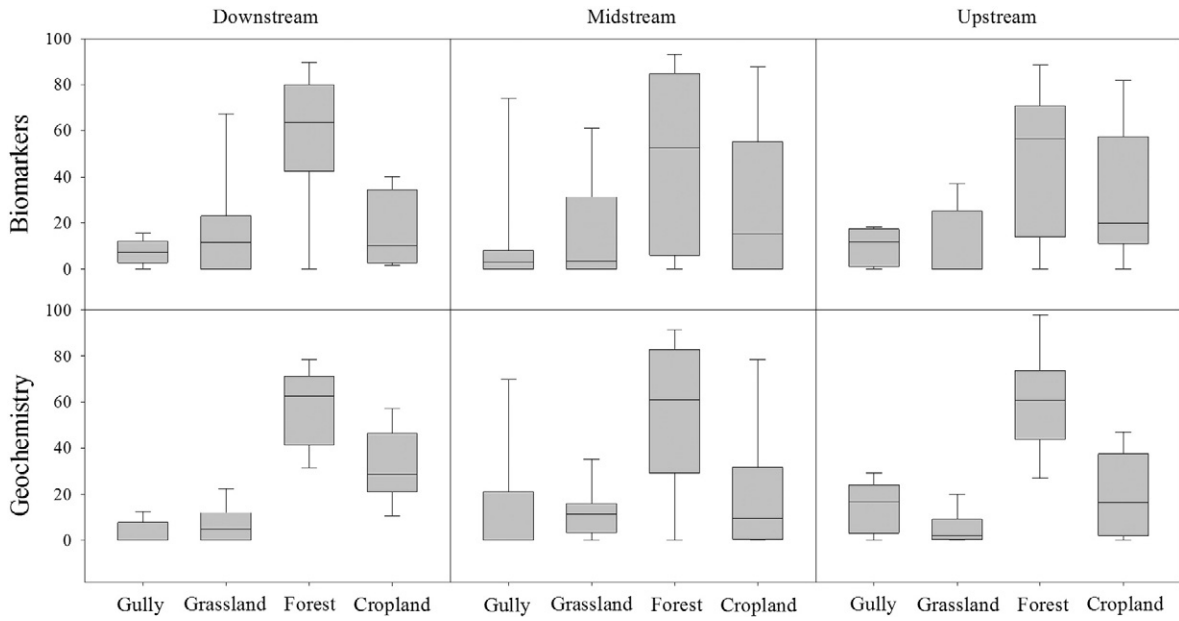
each of the four source types, and seven geochemical properties (i.e., Mg, Ti, Sc, Pb, U, Y, and Zr) were used to create a composite fingerprint with a predictive power of 90.0% (Table 4). CPI was the most important fingerprint factors which had a highest predictive power of 67.7%. The different source types had different classification accuracies. For the biomarkers, 80.0% of the gully and grassland samples were classified correctly, and 86.7% and 100.0% of the forest and cropland samples were classified correctly, respectively. For the geochemical properties, 86.7%, 100.0%, 80.0%, and 93.3% of the gully, grassland, forest, and cropland samples were classified correctly, respectively. In this catchment, the mean concentrations of the organic matter in four potential sediment sources (forest, grassland, cropland and gully) were 26.1, 13.4, 8.4, and 3.7 g/kg, respectively. The results of the organic matters were consistent with the other researches in Loess Plateau (Fu et al., 2000). The concentrations of organic matters may influence the source classification accuracy of biomarkers. Lipids only make up a

Fig. 4. Average sediment contributions of two fingerprint properties in the catchment (downstream portion (A1–A3), midstream portion (A4–A6) and upstream portion (A7–A9) of the check dam).
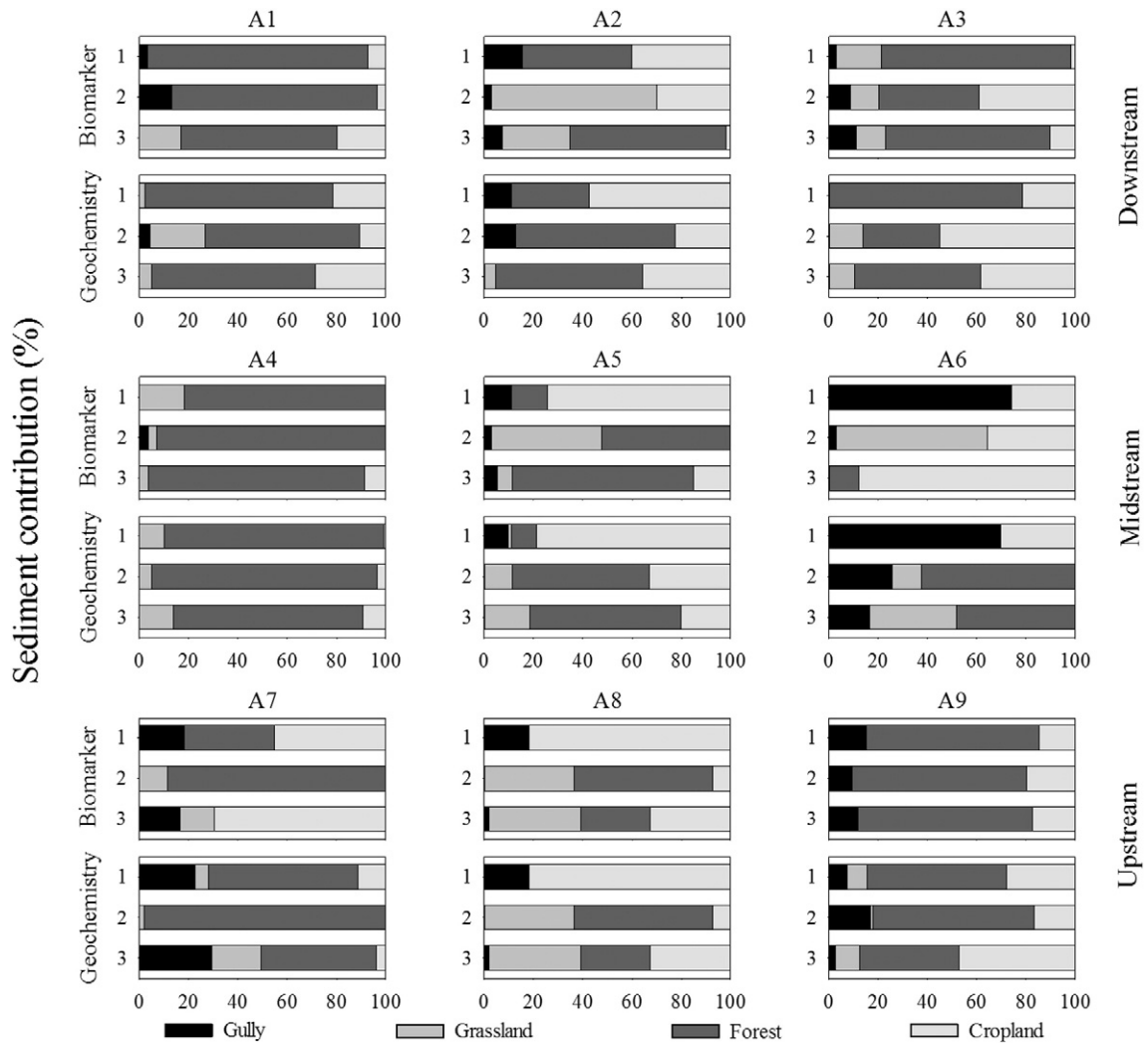

Fig. 5. Sediment contribution details for each profile from two fingerprint properties (1, 2, and 3 mark the flood couplets).

sediment contributions demonstrated the temporal heterogeneity of soil erosion (Renschler et al., 1999; Renschler and Harbor, 2002).

In the studied catchment, both geochemical properties and biomarkers indicated that forests contributed more than half of the sediments (Figs. 4 and 5), this result was consistent with the result of *n*-alkanes distribution in sediments. However, surface soils of forests are not likely to represent a significant sediment source nor contribute much sediment (Collins et al., 2010, 2012a, 2012b), in the artificial forests, the certain geography, underlying surface and hydrological conditions may be not capable of preventing erosion completely. First, these forests cover a large area (62.3% of the catchment), and the average surface gradient (15.1°) in the forests is greater than the average gradient (14.1°) throughout the catchment; soil erosion thus becomes more intense as the gradient increases (Shi and Shao, 2000; Fu et al., 2009). Second, the leaves of *R. pseudoacacia* were very small and thin; the leaf litter and understory were poorly developed, thus creating bare topsoil in the forest, which would cause serious soil erosion (Fu et al., 2009; J'i et al., 2009). Third, poor infiltrability in artificial forests induced surface runoff increase, which would induce soil erosion increase (Chen et al., 2007), and the eroding forest surfaces may be well connected to the stream network in this system. In the Hujiawan catchment, the loose topsoil in the cropland was prone to erosion when erosive rainfall events occurred, cropland accounts for only 6.7% of the study area, but it contributed more than 20% of sediments in both biomarker and geochemistry models. Fu et al. (2009) indicated that cropland usually has a high erosion rate because of tillage, and the majority of the croplands in this study area were located near the check dam (Fig. 2). Thus, the sediments would be expected to travel rapidly from the summit to the toeslope and follow a straight path to the check dam.

As shown in Fig. 5, the sediment contributions in the nine soil profiles and each flood couplets are clearly visible. The results indicated that the gully contributed small proportions (Figs. 4 and 5). Juracek and Ziegler (2009) indicated that erosion in the gullies typically decreased when the in-stream sediment loads were large. Therefore, in the whole gully systems, the erosion would be weakened because the surface runoff had been carried amounts of sediments which derived from forest and cropland. In addition, the sediment derived from the upstream gullies may deposit within downstream gullies where the landform was flat or where the slope gradient decreased and the width of the gully increased (Walling, 1983). In a comparison of biomarker and geochemical fingerprinting data, the result of former was larger than the latter by almost 75% in grassland sediments. Usually, grassland may have significantly reduced soil erosion (e.g., the result of geochemical fingerprinting data) (Ludwig et al., 2005; Fu et al., 2009). However, Blake et al. (2012) reported that the geochemical fingerprinting data overestimated cultivated land inputs to catchment sediment yields because of an inability to discriminate temporary pastures (in rotation) from cultivated land. In this catchment, a history of mixed land use (e.g., forest and grassland) would reduce discrimination between soil source. Meanwhile, forests had the lowest classification accuracy (80.0%) according to the geochemical fingerprinting data; the forest inputs to the catchment sediment yields may have been overestimated because of an inability to discriminate grassland, Therefore, a part of forest sediments may be apportioned to grassland. But in general, the sediment contributions of two fingerprinting data in these four potential sources were similar.

However, there are some constrains of the method of biomarker fingerprinting. Koiter et al. (2013) indicated that biological activity can not only deplete an organic signal through decomposition (e.g., fatty acid would decompose in 1–2 weeks after the test soils were submerged, Gibbs (2008)), but sediments during their conveyance through the river basin may also acquire new and different organic properties such that they may no longer reflect their original source. It may mean biomarker fingerprinting is more suitable for small catchment (Blake et al., 2012). In the large study catchments, the sediments were more

likely to deposit and transform during the process of transportation (Walling, 1983; Motha et al., 2002). Therefore, the method of the biomarker fingerprintings should be applied in conjunction with conventional geochemical fingerprinting approaches (Blake et al., 2012; Hancock and Revill, 2013). In addition, the potential biomarker fingerprints were impacted by the sedimentary environments. The organic content of sediment transported within the riverine environments is composed of two components: (i) derived from the original source location (allochthonous component, e.g., land-plants (long-chain *n*-alkanes)); and (ii) derived from within the river (autochthonous component, e.g., algae, microbes (short-chain *n*-alkanes) and aquatic macrophytes (middle-chain *n*-alkanes)) (Meyers, 2003; Koiter et al., 2013). Most biogeochemical reactions that take place within the aquatic environment occur at phase discontinuities, such as sediment–water interfaces (Owens and Xu, 2011). Therefore, the short chain *n*-alkanes was not effective fingerprint factors, only middle and long chain *n*-alkanes could be used in this catchment. And if the sediments were in the water-rich environments (e.g., lacustrine, riverine and marine), the middle chain *n*-alkanes could not be used as fingerprint factors (e.g., only C_{27}–C_{31} was used, Cooper et al. (2015)). Sampling during the erosive rainfall events may resolve the situation which the potential fingerprint factors cannot be used. In addition, the biomarkers have been limited as long-term fingerprint factors in tracking sediment sources, while the land-use have changed (e.g., an agricultural catchment), the fingerprint factors in source soils would change with the plant species. In that case, the *n*-alkanes only can be considered as indicators to trace the sources of organic matters in sediments (Ficken et al., 2000; Meyers, 2003; Jeng, 2006; Fang et al., 2014), not as fingerprint factors to trace the sources of sediments. However, the geochemical fingerprinting could be used as long-term monitoring indicators of sediment sources (Franz et al., 2014; Chen et al., 2016).

The biomarkers in sediment fingerprinting studies have the potential to provide better spatial constraints for sediment sources compared to other fingerprint properties, and/or differentiate between sources that other, more conventional, properties are unable to (McConnachie and Petticrew, 2006; Granger et al., 2007, Koiter et al., 2013). For example, geochemical properties have been studied to differentiate between broad categories of sediment sources (Collins et al., 2010, 2012a, 2012b), and cannot provide crucial crop-specific information on sediment source which represents a major shortcoming. Such data may not be of sufficient detail for river basin managers to make effective and well informed decisions. In contrast, *n*-alkanes have the potential to discriminate between a greater number and different land-use types of sediment sources (e.g., between different crops and trees) and provide greater detail regarding sediment sources on the scales of a small catchment.

4. Conclusions

The majority of existing fingerprinting studies have focused solely on inorganic sediment provenance, and the apportionment of organic matter in sediments remains largely undeveloped. This study used the composite fingerprinting method and new fingerprint properties (individual *n*-alkanes) to identify sediment sources in a small catchment. The new fingerprint featured properties that depended on the land use/cover and resisted diagenetic modifications and degradation. However, because of the activities of microbes, only the middle and long chain *n*-alkanes could be used as effective fingerprints in check dam. The optimal composite fingerprint consisted of a total of 6 individual properties (CPI, OEP_M, C_{28}, C_{21}, C_{24}, and C_{26}) and correctly distinguished 86.7% of the samples that were used to characterize each of the four source types. Meanwhile, the higher the concentration of biomarkers was, the higher the source classification accuracy became. The results demonstrated that young forest is the main sediment source in this catchment, i.e., 50.5%, and cropland, grassland, and gully contributed 25.6%, 14.4%, and 9.5% of the sediment, respectively. Variations in hydrodynamic conditions can result in different sediment fraction

distributions in different parts of the check dam. The forest and grassland contribution gradually increased from upstream to downstream, and the sediment contributions of cropland gradually decreased in the direction of the runoff pathway. Cropland also displayed high erosion rates because of tillage. In a comparison of biomarker and geochemical fingerprinting data, the latter may overestimated forest inputs to catchment sediment yields because of a mixed land use history (i.e., forest and grassland). Although shortcomings in the geochemical fingerprint approach limit its ability to fully discriminate sources based on land management regimes, *n*-alkanes have the potential to discriminate between a greater number and different types of sediment sources (e.g., between different crop types or tree species) and provide greater detail regarding sediment sources.

Conflict of interest statement

We declare that we have no financial and personal relationships with other people or organizations that can inappropriately influence our work, there is no professional or other personal interest of any nature or kind in any product, service and/or company that could be construed as influencing the position presented in, or the review of, the manuscript entitled.

Acknowledgements

References

Blake, W.H., Ficken, K.J., Taylor, P., Russell, M.A., Walling, D.E., 2012. Tracing crop-specific sediment sources in agricultural catchments. Geomorphology 139-140, 322–329.

Brincat, D., Yamada, K., Ishiwatari, R., Uemura, H., Naraoka, H., 2000. Molecular-isotopic stratigraphy of long-chain *n*-alkanes in Lake Baikal Holocene and glacial age sediments. Org. Geochem. 31, 287–294.

Bull, I.D., Bergen, P.F., Nott, C.J., et al., 2000. Organic geochemical studies of soils from the Rothamsted classical experiments—V. The fate of lipids in different long-term experiments. Org. Geochem. 31, 389–408.

Chen, F.X., Zhang, F.B., Fang, N.F., et al., 2016. Sediment source analysis using the fingerprinting method in a small catchment of the Loess Plateau, China. J. Soils Sediments 1-15. http://dx.doi.org/10.1007/s11368-015-1336-7.

Chen, L.D., Huang, Z.L., Gong, J., Fu, B.J., Huang, Y.L., 2007. The effect of land cover/vegetation on soil water dynamic in the hilly area of the loess plateau. China. Catena 70 (2), 200–208.

Collins, A.L., Zhang, Y., McChesney, D., Walling, D.E., Haley, S.M., Smith, P., 2012b. Sediment source tracing in a lowland agricultural catchment in southern England using a modified procedure combining statistical analysis and numerical modelling. Sci. Total Environ. 414, 301–317.

Collins, A.L., Zhang, Y., Walling, D.E., Grenfell, S.E., Smith, P., Grischeff, J., Locke, A., Sweetapple, A., Brogden, D., 2012a. Quantifying fine-grained sediment sources in the River Axe catchment, southwest England: application of a Monte Carlo numerical modelling framework incorporating local and genetic algorithm optimisation. Hydrol. Process. 26, 1962–1983.

Collins, A.L., Walling, D.E., Leeks, G.J.L., 1997. Source type ascription for fluvial suspended sediment based on a quantitative composite fingerprinting technique. Catena 29, 1–27.

Collins, A.L., Walling, D.E., Webb, L., King, P., 2010. Apportioning catchment scale sediment sources using a modified composite fingerprinting technique incorporating property weightings and prior information. Geoderma 155, 249–261.

Cooper, R.J., Pedentchouk, N., Hiscock, K.M., Disdle, P., Krueger, T., Rawlins, B.G., 2015. Apportioning sources of organic matter in streambed sediments: an integrated molecular and compound-specific stable isotope approach. Sci. Total Environ. 520, 187–197.

Cranwell, P.A., 1973. Chain-length distribution of *n*-alkanes from lake sediments in relation to post-glacial environmental change. Freshw. Biol. 3, 259–265.

Davis, C.M., Fox, J.F., 2009. Sediment fingerprinting: review of the method and future improvements for allocating nonpoint source pollution. J. Environ. Eng. 135, 490–504.

Fang, J.D., Wu, F.C., Xiong, Y.Q., Li, F.S., Du, X.M., An, D., Wang, L.F., 2014. Source characterization of sedimentary organic matter using molecular and stable carbon isotopic composition of *n*-alkanes and fatty acids in sediment core from Lake Dianchi, China. Sci. Total Environ. 473-474, 410–421.

Fang, N.F., Shi, Z.H., Li, L, Guo, Z.L., Liu, Q.J., Ai, L, 2012. The effects of rainfall regimes and land use changes on runoff and soil loss in a small mountainous watershed. Catena 99, 1–8.

Ficken, K.J., Li, B., Swain, D.L., Eglinton, G., 2000. An *n*-alkane proxy for the sedimentary input of submerged/floating freshwater aquatic macrophytes. Org. Geochem. 31, 745–749.

Franz, C., Makeschin, F., Weiß, H., Lorz, C., 2014. Sediments in urban river basins: identification of sediment sources within the Lago Paranoa catchment, Brasilia DF, Brazil — using the fingerprint approach. Sci. Total Environ. 466-467, 513–523.

Fu, B.J., Chen, L.D., Ma, K.M., Zhou, H.F., Wang, J., 2000. The relationships between land use and soil conditions in the hilly area of the loess plateau in northern Shaanxi, China. Catena 39, 69–78.

Fu, B.J., Hu, C.X., Chen, L.D., Honnay, O., Gulinck, H., 2006. Evaluating change in agricultural landscape pattern between 1980 and 2000 in the Loess hilly region of Ansai County, China. Agric. Ecosyst. Environ. 114, 387–396.

Fu, B.J., Wang, Y.F., Lu, Y.H., He, C.S., Chen, L.D., Song, C.J., 2009. The effects of land-use combinations on soil erosion: a case study in the Loess Plateau of China. Prog. Phys. Geogr. 33, 793–804.

Gelpi, E., Schneider, H., Mann, J., Oro, J., 1970. Hydrocarbons of geochemical significance in microscopic algae. Phytochemistry 9 (3), 603–612.

Gibbs, M.M., 2008. Identifying source soils in contemporary estuarine sediments: a new compound-specific isotope method. Coasts 31 (2), 344–359.

Granger, S., Bol, R., Butler, P., Haygarth, P., Naden, P., Old, G., Owens, P., Smith, B., 2007. Processes affecting transfer of sediment and colloids, with associated phosphorus, from intensively farmed grasslands: tracing sediment and organic matter. Hydrol. Process. 21 (3), 417–422.

Guzmán, G., Quinton, J.N., Nearing, M.A., Mabit, L., Gómez, J.A., 2013. Sediment tracers in water erosion studies: current approaches and challenges. J. Soils Sediments 13 (4), 816–833.

Haddadchi, A., Ryder, D.S., Evrard, O., Olley, J., 2013. Sediment fingerprinting in fluvial systems: review of tracers, sediment sources and mixing models. Int. J. Sediment Res. 28, 560–578.

Han, J., McCarthy, E.D., Van Hoeven, W., Calvin, M., Bradley, W., 1968. Organic geochemical studies, II. A preliminary report on the distribution of aliphatic hydrocarbons in algae, in bacteria, and in a recent lake sediment. Proc. Natl. Acad. Sci. 59 (1), 29–33.

Hancock, G.J., Revill, A.T., 2013. Erosion source discrimination in a rural Australian catchment using compound-specific isotope analysis (CSIA). Hydrol. Process. 27, 923–932.

Hatfield, R.G., Maher, B.A., 2009. Fingerprinting upland sediment sources: particle size-specific magnetic linkages between soils, lake sediments and suspended sediments. Earth Surf. Process. Landf. 34, 1359–1373.

Ho, E.S., Meyers, P.A., 1994. Variability of early diagenesis in lake sediments: evidence from the sedimentary geolipid record in an isolated tarn. Chem. Geol. 112 (3), 309–324.

Hu, J.F., Peng, P.A., Fang, D.Y., Jia, G.D., Jian, Z.M., Wang, P.X., 2003. No aridity in Sunda Land during the Last Glaciation: evidence from molecular-isotopic stratigraphy of long-chain *n*-alkanes. Palaeogeogr. Palaeoclimatol. Palaeoecol. 201, 269–281.

Jeng, W.L., 2006. Higher plant *n-alkane* average chain length as an indicator of petrogenic hydrocarbon contamination in marine sediments. Mar. Chem. 102 (3–4), 242–251.

J'i, Ide, Kume, T., Wakiyama, Y., Higashi, N., Chiwa, M., Otsuki, K., 2009. Estimation of annual suspended sediment yield from a Japanese cypress (*Chamaecyparis obtusa*) plantation considering antecedent rainfalls. For. Ecol. Manag. 257, 1955–1965.

Juracek, K.E., Ziegler, A.C., 2009. Estimation of sediment sources using selected chemical tracers in the Perry lake basin, Kansas, USA. Int. J. Sediment Res. 24, 108–125.

Kimoto, A., Nearing, M.A., Shipitalo, M.J., Polyakov, V.O., 2006. Multi-year tracking of sediment sources in a small agricultural watershed using rare earth elements. Earth Surf. Process. Landf. 31, 1763–1774.

Koiter, A.J., Owens, P.N., Petticrew, E.L., Lobb, D.A., 2013. The behavioural characteristics of sediment properties and their implications for sediment fingerprinting as an approach for identifying sediment sources in river basins. Earth Sci. Rev. 125, 24–42.

Kolattukudy, P.E., Croteau, R., Buckner, J.S., 1976. Biochemistry of plant waxes. Chem. Biochemistry Nat. Wax. 290-349.

Liu, T.S., 1985. Loess and the Environment. Chinese Science Press, Beijing (in Chinese).

Ludwig, J.A., Wilcox, B.P., Breshears, D.D., Tongway, D.J., Imeson, A.C., 2005. Vegetation patches and runoff-erosion as interacting ecohydrological processes in semiarid landscapes. Ecology 86, 288–297.

Martínez-Carreras, N., Krein, A., Gallart, F., Iffly, J.F., Pfister, L., Hoffmann, L., Owens, P.N., 2010a. Assessment of different colour parameters for discriminating potential suspended sediment sources and provenance: a multi-scale study in Luxembourg. Geomorphology 118, 118–129.

Martínez-Carreras, N., Udelhoven, T., Krein, A., Gallart, F., Iffly, J.F., Ziebel, J., L., Hoffmann, Pfister, L., DE, Walling, 2010b. The use of sediment colour measured by diffuse reflectance spectrometry to determine sediment sources: application to the Attert River catchment (Luxembourg). J. Hydrol. 382, 49–63.

Matsumoto, K., Kawamura, K., Uchida, M., Shibata, Y., 2007. Radiocarbon content and stable carbon isotopic ratios of individual fatty acids in subsurface soil: implication for selective microbial degradation and modification of soil organic matter. Geochem. J. 41, 483–492.

McConnachie, J.L., Petticrew, E.L., 2006. Tracing organic matter sources in riverine suspended sediment: implications for fine sediment transfers. Geomorphology 79 (1–2), 13–26.

McKinley, R., Radcliffe, D., Mukundan, R., 2013. A streamlined approach for sediment source fingerprinting in a Southern Piedmont watershed, USA. J. Soils Sediments 13, 1754–1769.

Meyers, P.A., 1997. Organic geochemical proxies of paleoceanographic, paleolimnologic, and paleoclimatic processes. Org. Geochem. 27, 213–250.

Meyers, P.A., 2003. Applications of organic geochemistry to paleolimnological reconstructions: a summary of examples from the Laurentian Great Lakes. Org. Geochem. 34, 261–289.

Meyers, P.A., Ishiwatari, R., 1993. Lacustrine organic geochemistry—an overview of indicators of organic matter sources and diagenesis in lake sediments. Org. Geochem. 20, 867–900.

Motha, J., Wallbrink, P., Hairsine, P., Grayson, R., 2002. Tracer properties of eroded sediment and source material. Hydrol. Process. 16 (10), 1983–2000.

Owens, P.N., Xu, Z.H., 2011. Recent advances and future directions in soils and sediments research. J. Soils Sediments 6, 875–888.

Pancost, R.D., Boot, C.S., 2004. The palaeoclimatic utility of terrestrial biomarkers in marine sediments. Mar. Chem. 92 (1), 239–261.

Renschler, C.S., Harbor, J., 2002. Soil erosion assessment tools from point to regional scales—the role of geomorphologists in land management research and implementation. Geomorphology 47 (2), 189–209.

Renschler, C.S., Mannaerts, C., Diekkrüger, B., 1999. Evaluating spatial and temporal variability in soil erosion risk—rainfall erosivity and soil loss ratios in Andalusia. Spain. Catena 34 (3), 209–225.

Rogers, K.M., Collen, J.D., Johnston, J.H., Elgar, N.E., 1999. A geochemical appraisal of oil seeps from the East Coast Basin, New Zealand. Org. Geochem. 30, 593–605.

Rotman, R., Naylor, L., McDonnell, R., MacNiocaill, C., 2008. Sediment transport on the Freiston Shore managed realignment site: an investigation using environmental magnetism. Geomorphology 100, 241–255.

Shi, H., Shao, M.A., 2000. Soil and water loss from the Loess Plateau in China. J. Arid Environ. 45, 9–20.

Silva, T.R., Lopes, S.R.P., Spörl, G., Knoppers, B.A., Azevedo, D.A., 2012. Source characterization using molecular distribution and stable carbon isotopic composition of *n*-alkanes in sediment cores from the tropical Mundaú–Manguaba estuarine–lagoon system, Brazil. Org. Geochem. 53, 25–33.

Tareq, S.M., Tanoue, E., Tsuji, H., Tanaka, N., Ohta, K., 2005. Hydrocarbon and elemental carbon signatures in a tropical wetland: biogeochemical evidence of forest fire and vegetation changes. Chemosphere 59, 1655–1665.

Tsunekawa, A., Liu, G.B., Yamanaka, N., Du, S., 2014. Restoration and Development of the Degraded Loess Plateau. Springer, China.

Wallbrink, P.J., Murray, A.S., Olley, J.M., Olive, L.J., 1998. Determining sources and transit times of suspended sediment in the Murrumbidgee River, New South Wales, Australia, using fallout ^{137}Cs and [210]Pb. Water Resour. Res. 34, 879–887.

Walling, D.E., 1983. The sediment delivery problem. J. Hydrol. 65, 209–237.

Walling, D.E., 2005. Tracing suspended sediment sources in catchments and river systems. Sci. Total Environ. 344, 159–184.

Walling, D.E., 2013. The evolution of sediment source fingerprinting investigations in fluvial systems. J. Soils Sediments 13, 1658–1675.

Wang, Y.F., Chen, L.D., Fu, B.J., Lü, Y.H., 2014. Check dam sediments: an important indicator of the effects of environmental changes on soil erosion in the Loess Plateau in China. Environ. Monit. Assess. 186, 4275–4287.

Wilkinson, S.N., Hancock, G.J., Bartley, R., Hawdon, A.A., Keen, R.J., 2013. Using sediment tracing to assess processes and spatial patterns of erosion in grazed rangelands, Burdekin River basin, Australia. Agric. Ecosyst. Environ. 180, 90–102.

Yang, M.Y., Tian, J.L., Liu, P.L., 2006. Investigating the spatial distribution of soil erosion and deposition in a small catchment on the Loess Plateau of China, using [137]Cs. Soil Tillage Res. 87, 186–193.

Zech, M., Krause, T., Meszner, S., Faust, D., 2013. Incorrect when uncorrected: reconstructing vegetation history using *n*-alkane biomarkers in loess-paleosol sequences — a case study from the Saxonian loess region, Germany. Quat. Int. 296, 108–116.

Zech, M., Rass, S., Buggle, B., Löscher, M., Zöller, L., 2012. Reconstruction of the late Quaternary paleoenvironments of the Nussloch loess paleosol sequence, Germany, using *n*-alkane biomarkers. Quat. Res. 78, 226–235.

Zhang, X., Li, Z.W., Tang, Z.H., Zeng, G.M., Huang, J.Q., Guo, W., Chen, X.L., Hirsh, A., 2013. Effects of water erosion on the redistribution of soil organic carbon in the hilly red soil region of southern China. Geomorphology 197, 137–144.

Zhao, M.X., Dupont, L., Eglinton, G., Teece, M., 2003. *n*-Alkane and pollen reconstruction of terrestrial climate and vegetation for N.W. Africa over the last 160 kyr. Org. Geochem. 34, 131–143.

Zheng, Y.H., Zhou, W.J., Meyers, P.A., Xie, S.C., 2007. Lipid biomarkers in the Zoigê-Hongyuan peat deposit: indicators of Holocene climate changes in West China. Org. Geochem. 38, 1927–1940.